5-2008

Optical properties of colloidal core/shell nanocrystals

Abhishek Joshi
University of Arkansas, Fayetteville

OPTICAL PROPERTIES OF COLLOIDAL CORE/SHELL NANOCRYSTALS

OPTICAL PROPERTIES OF COLLOIDAL CORE/SHELL NANOCRYSTALS

A thesis submitted in partial fulfillment
of the requirements for the degree
of Bachelor of Science (Honors) in
Electrical Engineering

By

Abhishek Joshi

May 2008
University of Arkansas

Abstract

Recently, colloidal core/shell nanocrystals have found use in several applications such as solar cells, light emitting diodes, fluorescent dies, etc. In this thesis, optical properties of colloidal CdSe/ZnS core/shell nanocrystals were studied. The samples were prepared such that the nanocrystals were embedded in a UV curable resin. Once the samples were cured, they were placed in different spectrophotometers to measure the absorbance and the photoluminescence (PL) spectrum. The effect on the absorbance and PL spectra was investigated by using nanocrystal samples of different quantum dot sizes and by changing the temperature of the samples.

It was found that the energy band gap of the nanocrystal structures tends to increase as the nanocrystal diameter decreases. The energy band gap also decreases as the temperature of the nanocrystal sample increases. The Stokes shift (the difference between the absorbance and PL peaks) was found to increase as the nanocrystal diameter decreases. Through calculations, it was determined that the electron-phonon coupling increases as the nanocrystal diameter decreases. Finally, Debye and Einstein temperatures are calculated analytically and their ratio was found to be close to unity.

Acknowledgements

I would like to thank my honors thesis advisor, Dr. Omar Manasreh for his support, enthusiasm and motivation throughout my undergraduate years. I would like to thank him for giving me the opportunity to work in the *Optoelectronics and Nanostructures Lab* and I would also like to thank all of the lab members from whom I always had the opportunity to learn something new.

Words can not express the gratitude I have for my Ma and Pa. They have given me unconditional love and support throughout these years and I thank them for giving me the inspiration to look forward and succeed.

Table of Contents

List of Figures

List of Tables

1. Introduction

1.1 Electronic structure of atoms

1.1.1 The Photoelectric Effect

When studying blackbody radiation, Planck made an important observation that radiation energy absorbed or emitted by the body was not continuous but in discrete units called *quanta*. Each unit of energy E, called quantum, can be found by the following equation [1]:

$$E = \hbar \nu$$

where, ħ = 6.63 X 10^{-34} J-s (Planck's constant)

ν = frequency of the radiation

1.1.2 Electron Models

Optical properties of materials such as emission spectra can be described by the use of electron models. One of the earliest electron models was the Bohr model of the Hydrogen atom. Some of the postulates were:

- Electrons exist in stable circular orbits about the nucleus just like the planetary solar system.
- The electron can shift to an orbit of higher or lower energy by losing or gaining energy equivalent to the difference in the energy levels. This energy is not continuous but in discrete finite amounts of quanta.

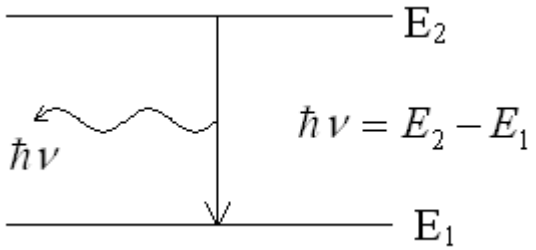

1.1.3 Semiconductor Energy Bands

In solids, the electrons in an atom can be viewed as existing in different bands of energies. For example, a Silicon atom, Si_{14} has the following electron structure: $1s^2 2s^2 2p^6 3s^2 3p^2$. The outer shell (n=3) is composed of 4 electrons: 2 in 3s energy level and 2 in 3p energy level. The entire (n=3) band can contain a maximum of 8 electrons. In a solid structure such as a Si wafer, the band splits into two bands: Conduction band (E_C) which is the upper band and Valence Band (E_V) which is the lower band. These two bands of energy levels are separated by a forbidden zone called the Energy Band gap (E_g). An electron can exist in E_C or E_V but not in E_g.

There are two classes of semiconductors based on energy bands: direct and indirect.

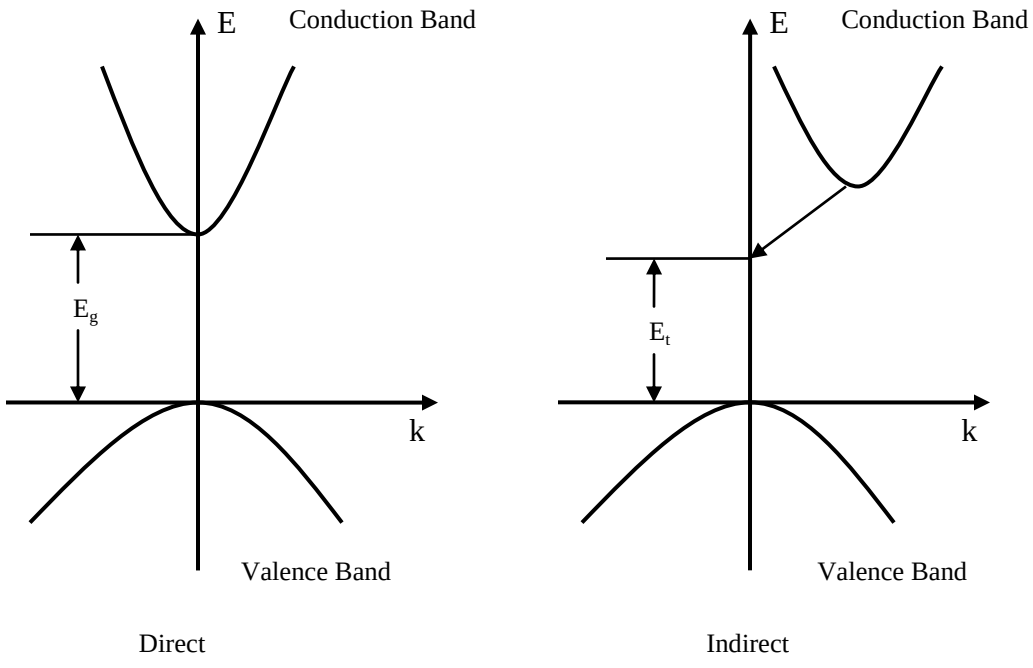

Figure 1.1 Direct and Indirect Electron Transitions in Semiconductor

Figure 1 shows the difference in the energy levels in the direct and indirect semiconductor materials. When enough energy is supplied to an electron in the valence band, it will cross the energy band gap and reach the conduction band. The *electron* in the conduction band has created a vacancy in the valence band and this vacancy is called a *hole*. In a direct semiconductor such as GaAs, an electron in the conduction band can transition directly to an empty state in the valence band giving off a photon equivalent to the energy band gap E_g. On the other hand, in an indirect semiconductor such as Si, an electron in the conduction band can not transition directly to the valence band, but has to undergo a change in the momentum and energy to reach an empty valence band state. In Figure 1, the electron passes through a defect state (E_t) before transitioning into the valence band [1].

1.2 Nanocrystals

1.2.1 Concept of Nanocrystals

When semiconductor material goes down from wafer-level (bulk) scale to a scale of a few atoms or few hundred atoms, the properties are markedly different. These clusters or particles have different electronic spectra, optical properties, etc compared to bulk material. These clusters are generally larger than the crystal lattice constant but are comparable to the de Broglie wavelength of the elementary excitations. They are often called as “quantum crystallites” or “quantum dots” or “nanocrystals.” Since the size of these crystallites ranges from a few nanometers to a few hundred nanometers, they are called Nanocrystals [3].

1.2.2 Structure of Nanocrystals

A way to model the structure of nanocrystal material is to consider it as a "semiconductor inclusion embedded in an insulating matrix." [4] Figure 2 shows the potential well formed in any of the three dimensions (x,y,z) in the conduction and valence bands. In this three-dimensional well, the conduction and the valence bands are quantized into discrete hole and electron levels respectively because of the finite size of the nanocrystal cluster.

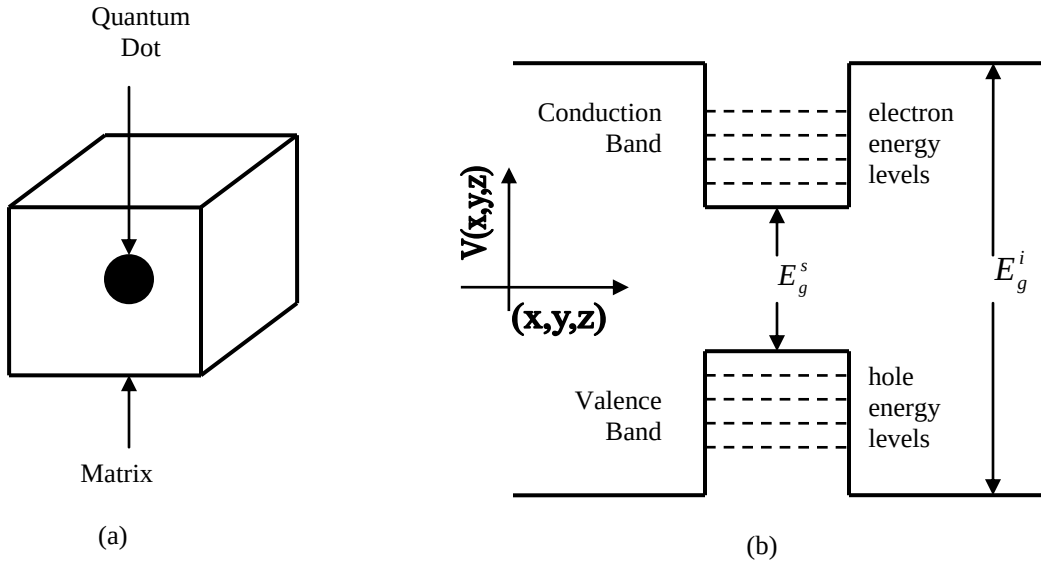

Figure 1.2 (a) Simple model of a nanocrystal as a quantum dot embedded in a insulating matrix (b) Potential well formed in any dimension (x,y,z) in the conduction and valence bands

1.3 Scope of this Thesis

1.3.1 Motivation

It has been observed that when the nanocrystal size reaches comparable levels to the natural length limit of the electron-hole pair, i.e., the exciton Bohr radius, different optical properties are observed for different sizes of nanocrystal particles [5-6]. In this limit, also known as the strong confinement regime [5], the electron and hole wave functions become confined in all three dimensions due to the finite dot boundary. Such confinement leads to the quantization of the electronic bands (as explained in the previous section) and discrete optical transition spectra has been observed for different nanocrystal sizes, such as CdSe [7].

Recently, there has been a lot of interest in the II-VI semiconductor nanocrystals due to their use in several different optoelectronic applications such as solar cells [8-9] and light-emitting diodes [10]. Core/shell nanocrystals such as CdSe/ZnS produced by colloidal growth are being investigated because they exhibit different optical properties, such as photoluminescence (emission spectra) and absorption spectra for different nanocrystal sizes.

1.3.2 Goal of this work

The goal of this research work is to report the temperature dependence of the photoluminescence and absorption spectra measurements for different sizes of CdSe/ZnS core/shell colloidal nanocrystals embedded in a UV curable resin. Different samples were created and optical spectra were recorded in the temperature range of 10 – 300K. Debye and Einstein temperatures were calculated from the measurements and the Stokes shift was estimated for nanocrystal samples with different diameters.

1.3.3 Organization of this work

Chapter 2 provides a brief background in core/shell nanocrystals. It also describes the structure of the core/shell nanocrystals and the different nanocrystal types used in this research work.

Chapter 3 describes in detail the setup of the experiment, the types of tools used to measure the optical spectra and a brief description of the way the experiments were carried out.

Chapter 4 presents the results obtained from the set of experiments and attempts to give a discussion of this work and the way it this work correlates with the related research efforts in this area.

Chapter 5 ends this report by drawing conclusions out from this work and raises some possibilities on further research in this area.

2. Background

2.1 Core/shell nanocrystals

2.1.1 Structure

In this research work, CdSe/ZnS core/shell nanocrystals produced by colloidal growth techniques from Evident Technologies were used for investigation [11]. The structure of a typical CdSe/ZnS core/shell nanocrystal is shown in Figure 3.

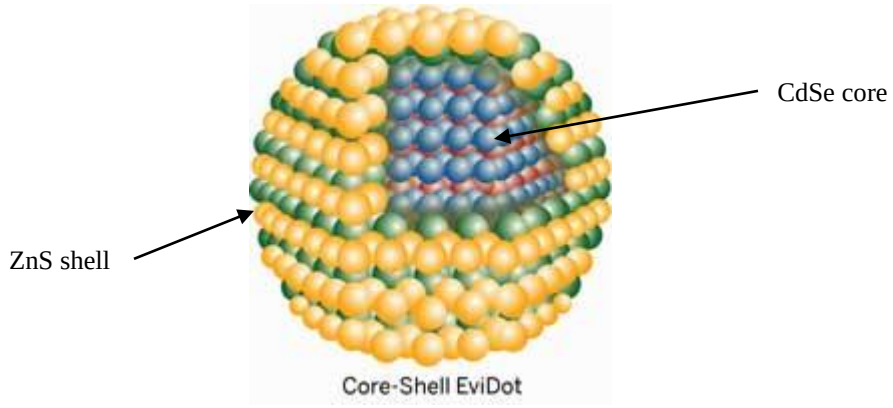

Figure 2.1 A CdSe/ZnS core/shell nanocrystal structure [Courtesy of Ref. 11]

A core/shell nanocrystal can be considered as similar to an egg structure in which the outer shell is composed of ZnS and the inner yolk is composed to CdSe.

2.1.2 Types of Nanocrystals

Several different types of nanocrystal material with different diameters and first exciton spectra were used. Table 1 summarizes the types of CdSe/ZnS nanocrystals based on the diameter, the emission peak wavelengths and the first exciton peak wavelengths.

Emission Peak [nm]	First Exciton Peak [nm-nominal]	Crystal Diameter [nm-approx]	Molecular Weight [µg/nmol]
490	470	3.2	85
520	500	3.3	94
540	520	3.4	100
560	540	3.8	140
580	560	4.4	200
600	580	5.0	270
620	600	5.8	400

Table 2.1 Summary of different CdSe/ZnS core/shell nanocrystals used for this work

The characteristic absorption spectrum for these nanocrystals is shown in Figure 2.2.

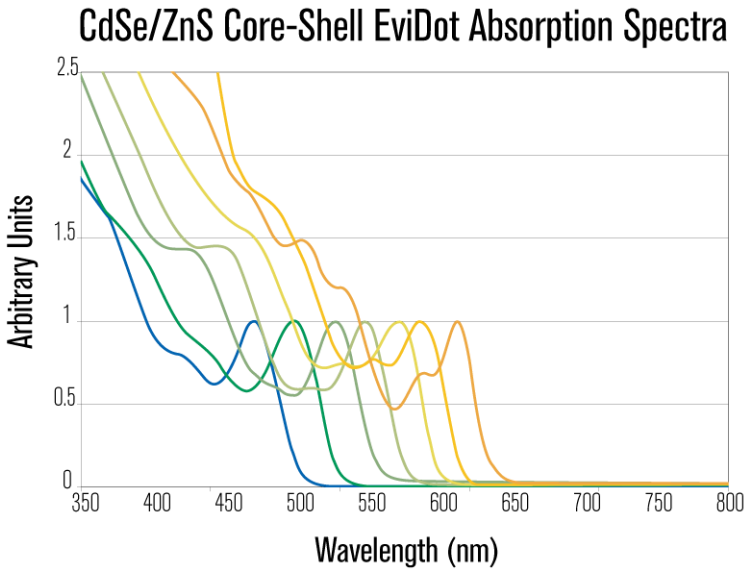

Figure 2.2 Manufacturer specified CdSe/ZnS nanocrystal absorption spectra [Courtesy of Ref. 11]

From Fig. 2.2, it is apparent that as the nanocrystal diameter increases, the peak of the absorption spectrum increases in wavelength or shifts towards right. The characteristic emission spectrum for these nanocrystals is shown in Figure 2.3. From this plot, it is also apparent that as the diameter of the nanocrystals increases, the peak of the emission spectrum wavelength increases or shifts towards right as well.

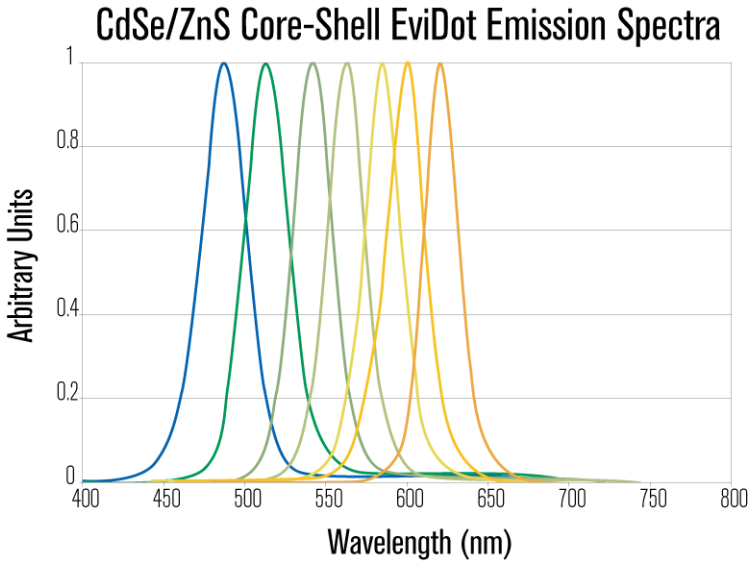

Figure 2.3 Manufacturer specified CdSe/ZnS nanocrystal emission spectra [Courtesy of Ref. 11]

These colloidal CdSe/ZnS nanocrystals were obtained in a UV curable polyurethane oligomer/acrylic acid resin.

3. Experimental Setup

3.1 Sample Preparation

To be able to take record optical spectra, the nanocrystals need to be restrained in an effective manner so that the absorbed or the emitted radiation can be measured. One of the main challenges faced is to find a way to matrix these nanocrystal quantum dots into some type of resin in which the nanocrystals will stay embedded there in. For these set of experiments, the CdSe/ZnS nanocrystal material was mixed with a UV curable resin and the resulting composite was deposited upon c-plane sapphire substrate pieces. Each sapphire substrate piece was about 1.0 cm X 1.0 cm in area. Care was taken to ensure that the resulting cross-section surface was as horizontal as possible and not convex as that can induce errors in the measurements. After the composite was deposited, the samples were initially left alone for the resin to spread to the edges and set down in the substrate properly. Then the samples were placed under a 200W UV light for 90 minutes. After the exposure, the samples were cured and the nanocrystal material was effectively restrained in place and in a way was shielded from dust particles. Since the sample was cured, it can now be used for temperature dependent measurements too.

3.2 Absorption Spectra Measurement with the Cary 500 spectrometer

The Varian Cary 500 spectrometer in conjunction with a closed-cycle refrigeration system is used to measure the optical absorption spectra of the nanocrystals. The existence of a closed cycle refrigeration system gives the ability to control the sample temperature from 10 – 300K to accuracy within ±1.0K. An image of the Varian Cary 500 system is shown in Figure 3.1.

Figure 3.1 The Varian Cary 500 spectrometer

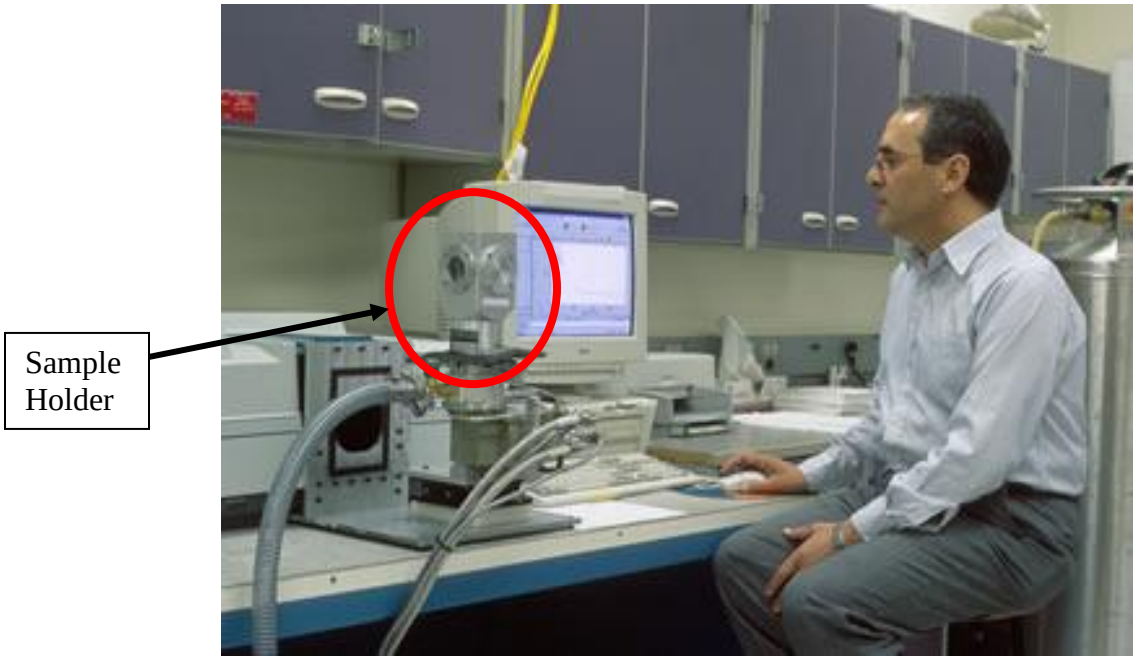

Figure 3.2 The sample holder for the Varian Cary 500 spectrometer

The sample is secured by using a double-sided tape on the edge of the sample. It is imperative that the tape does not the cover the hole through which the incident light will

pass through. Otherwise, the absorbance will incorrectly contain the spectrum of the plastic tape. An image of the sample holder is shown in Figure 3.2.

The Cary 500 spectrophotometer works by doing a frequency sweep of the generated light, i.e., it starts at 175 nm and gradually increases the wavelength of the incident light all the way until the maximum limit of 3200 nm. A light source generates the incident light which passes through the external sample holder windows, the sample, and though the hole in the mounting finger before reaching the detector on the other end. The sample holder has two sapphire windows. Therefore, the resulting absorbance spectrum actually includes the absorbance spectrum of sapphire crystal in conjunction with the nanocrystal spectrum.

To void such errors in measurement, a baseline measurement is run without any sample in the sample holder. Since the spectra can shift with respect to temperature, humidity and other atmospheric conditions, the baseline measurement is run once at the start of each set of experiments. Once the base line measurement has been recorded, the actual nanocrystal measurements can be run and the base line measurements are automatically subtracted by the Cary WinUV program.

To measure temperature dependence of the absorbance spectrum, the closed-cycle refrigerator system is run in conjunction with the Cary 500 setup. Because the sample can actually reach temperatures close to 10K, the double-sided tape solution will fail. In such case, a vacuum adhesive gel mixed with Silver (Ag) is applied near the edges of the sapphire base to secure the sample properly. For proper measurements, the vacuum pressure is required to be below 10^{-5} torr. To ensure the consistency of measurements, the temperature starts at 300K (room temperature), an absorbance spectrum is recorded, then

the temperature is decreased by a step of 10K, then given at least 3 minutes to settle, an absorbance spectrum is recorded, then the temperature decreased by a step of 10K and the whole process is repeated until the temperature reaches 10K. In some cases, for verification, the temperature is again raised by a step of 10K, the corresponding absorbance spectrum is measured and the process is repeated again until the temperature reaches 300K.

3.3 Photoluminescence (PL) Spectra Measurement with the Bomem DA8 spectrometer

The Bomem DA8 Fourier Transform Infrared (FTIR) spectrophotometer with a continuous-flow cryostat is used to measure the photoluminescence (PL) or the emission spectrum from the core/shell nanocrystals. This arrangement allows Liquid Nitrogen (77K) to be poured into the cryostat to cool down the nanocrystal samples and observe the corresponding changes in the emission spectrum. An image of the DA8 is shown in Figure 3.3.

Figure 3.3 The Bomem DA8 FTIR spectrophotometer

Unlike the Cary 500 sample holder which allows only one sample to be secured, the DA8 sample holder allows five samples to be mounted at a time. The advantages are clearly obvious: Less time to mount and de-mount the samples and less susceptibility of errors in measurement due to changes in the lab environment. Since the spectrum being recorded is the emission spectrum, there is no need for a hole to allow the refracted light to be sensed by a detector. Therefore, instead of a tape, the vacuum gel is used over the entire backside of the sapphire plane to secure the sample properly to the mounting finger.

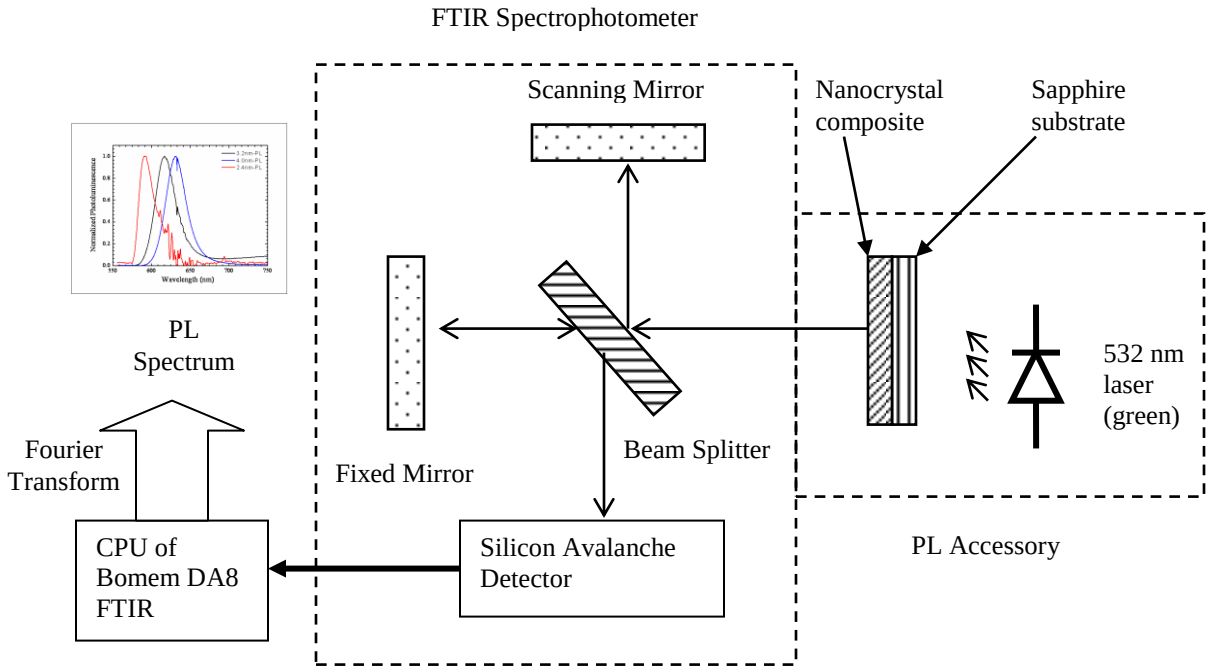

Figure 3.4 Schematic diagram of the Bomem DA8 Spectrophotometer

A schematic diagram of the Bomem DA8 is presented in Figure 3.4 to explain the operating functionality. The light is generated by a cw green (532 nm) laser and with the assistance of the fixed and scanning mirrors, the light emitted from the nanocrystal

samples is separated from the incident light by the beam splitter. The Silicon Avalanche detector converts the emission signal and sends it to the CPU of the spectrophotometer. Resident software computes the Fast Fourier Transform (FFT) to display the photoluminescence spectrum against wavelength. As the tool accessory allows multiple samples to be loaded at once, multiple PL results can be recorded in one set of experiments.

4. Results & Discussion

4.1 Absorbance Spectra

In this study, four CdSe/ZnS core/shell nanocrystal samples were studied with crystal diameters of approximately 4.0, 3.2, 2.4 and 1.9 nm. The lowest peak in the absorption spectra is generally referred to as the first exciton peak. It was observed that these nanocrystal samples exhibit their first exciton peaks at 600, 580, 520, and 475 nm in units of wavelength, respectively. The normalized absorbance spectra measured for the four samples at room temperature (300K) are shown in Fig. 4.1.

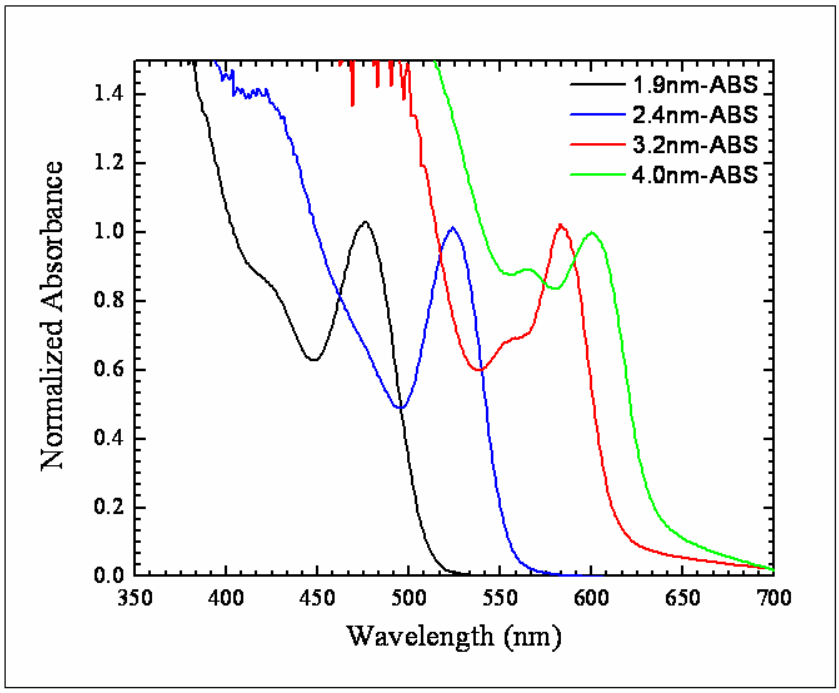

Figure 4.1 Normalized absorption spectra plotted as a function of the wavelength of the incident light.

It can be inferred that as the nanocrystal diameter decreases, the wavelengths corresponding to the first exciton peaks shift toward left, i.e., exhibit a blue-shift property.

4.2 Photoluminescence Spectra

The photoluminescence (PL) or the emission spectra were obtained for three types of CdSe/ZnS core/shell nanocrystals with diameters of 2.4, 3.2 and 4.0 nm at 300K. The corresponding first exciton peaks are shown in Figure 4.2.

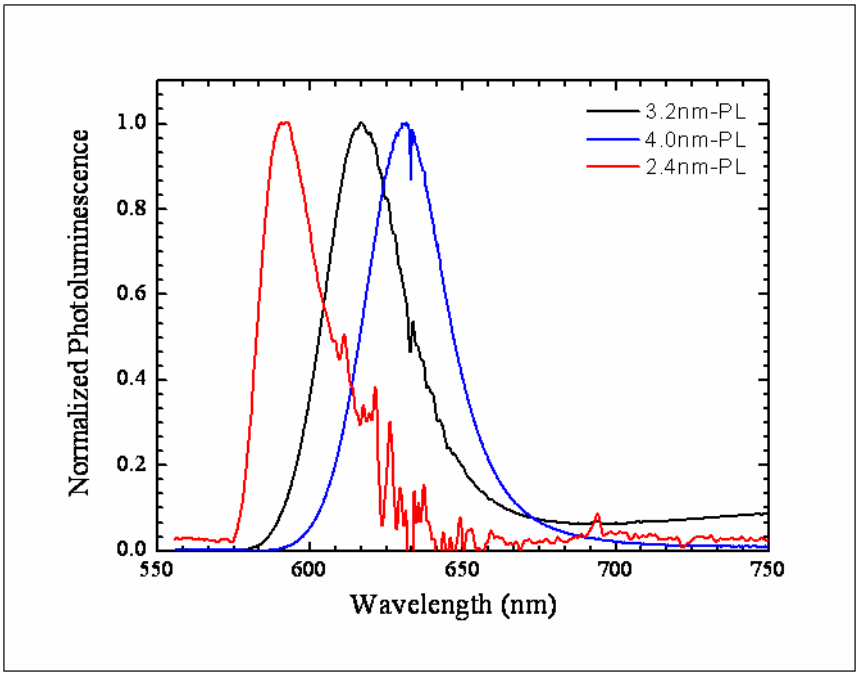

Figure 4.2 Normalized PL spectra plotted as a function of wavelength for three samples

As was described in the previous section, the incident light beam is generated by a green laser (532 nm wavelength). The emission spectrum that comes from the nanocrystal sample has a strong component in the 532 nm region. A notch filter (at about 532 nm region) is used to filter out the strong laser component. However, the PL spectrum of the 1.8 nm nanocrystal is centered on the 532 nm region and hence is cutoff inherently. Because of the limitation in the tool's capability to record the PL spectrum properly, the results from the nanocrystal sample with diameter 1.8 nm was not shown as half of the spectrum was not displayed. The line at 632 nm is due to the HeNe red laser

used for the spectrometer dynamic alignment [12]. From Fig. 4.2, it is apparent that as the nanocrystal diameter decreases, there is a blue-shift in the wavelengths corresponding to the first exciton peak in the PL spectra.

4.3 Energy band gap (E_g) as a function of NC Diameter

The energy band gap in this study is defined as the energy of the first exciton peak in the absorption spectra. A plot of the energy band gap (E_g) as a function of the nanocrystal diameter is shown in Figure 4.3.

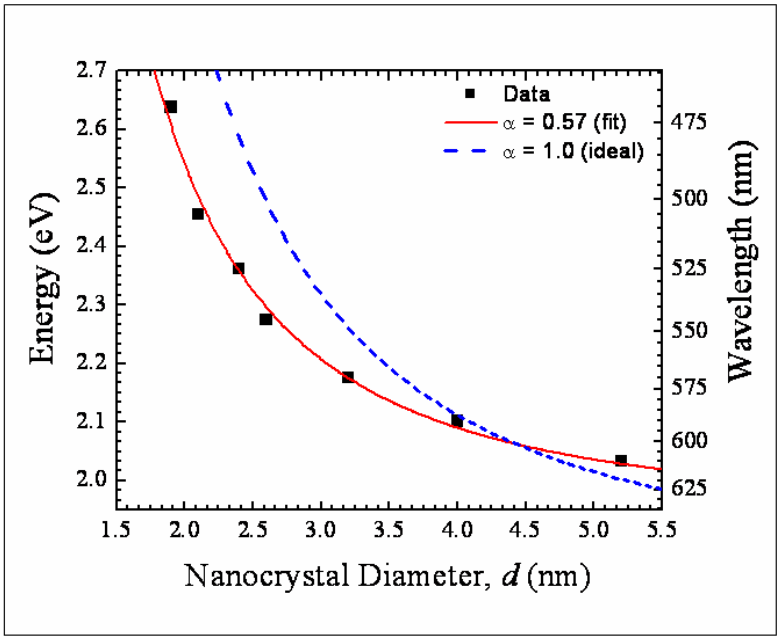

Figure 4.3 Energy band gap plotted as a function of the nanocrystal diameter (solid squares). The solid line represents the case for α = 0.57 and the dashed line represents the case for α = 1.0.

The energy band gap as a function of the nanocrystal diameter is fitted with the following relation [2]:

$$E = E_g + \alpha\left(\frac{\pi^2\hbar^2}{2\mu^* d^2}\right)$$

where, E_g is the energy band gap (eV) of the bulk semiconductor material, α is a fitting parameter related to the distribution of the nanocrystal size, ħ is the Planck's constant, d is the nanocrystal diameter and μ^* is the reduced effective mass. The red solid line in Figure 4.3 is the fit for the data (represented by the above equation). From this fit, it was found that α = 0.57 and E_g = 1.938 eV. The ideal case is for bulk semiconductor material where α = 1.0 and bulk E_g = 1.845 eV. In such an ideal case, all of the nanocrystals have the same diameter and the curve for the ideal case is represented by the blue dashed line in Fig. 4.3.

4.4 The Stokes shift

The absorbance and the PL spectra are plotted together in the same graph for nanocrystals with diameter 2.4, 3.2 and 4.0 nm. Figure 4.4 displays the absorbance and PL spectra for the 2.4 nm diameter CdSe/ZnS core/shell nanocrystal type.

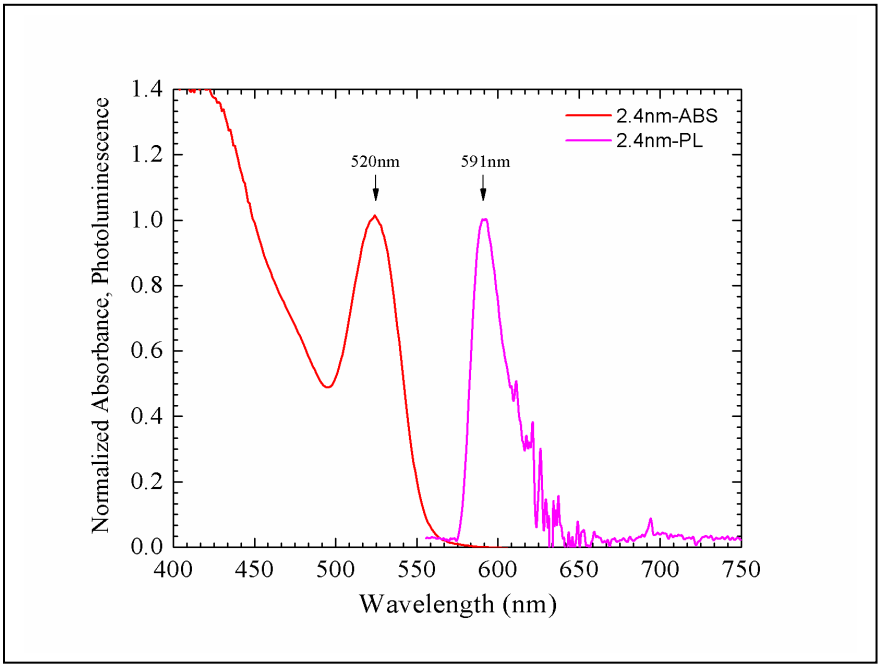

Figure 4.4 Normalized PL and absorption spectra are plotted together for the 2.4 nm nanocrystal diameter. The corresponding emission and the exciton peaks are labeled.

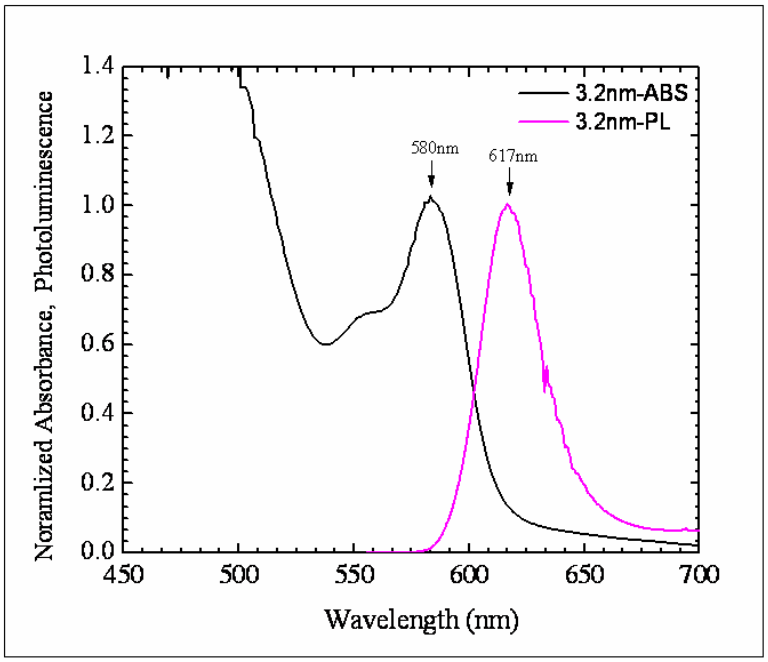

Figure 4.5 Normalized PL and absorption spectra are plotted together for the 3.2 nm nanocrystal diameter. The corresponding emission and the exciton peaks are labeled.

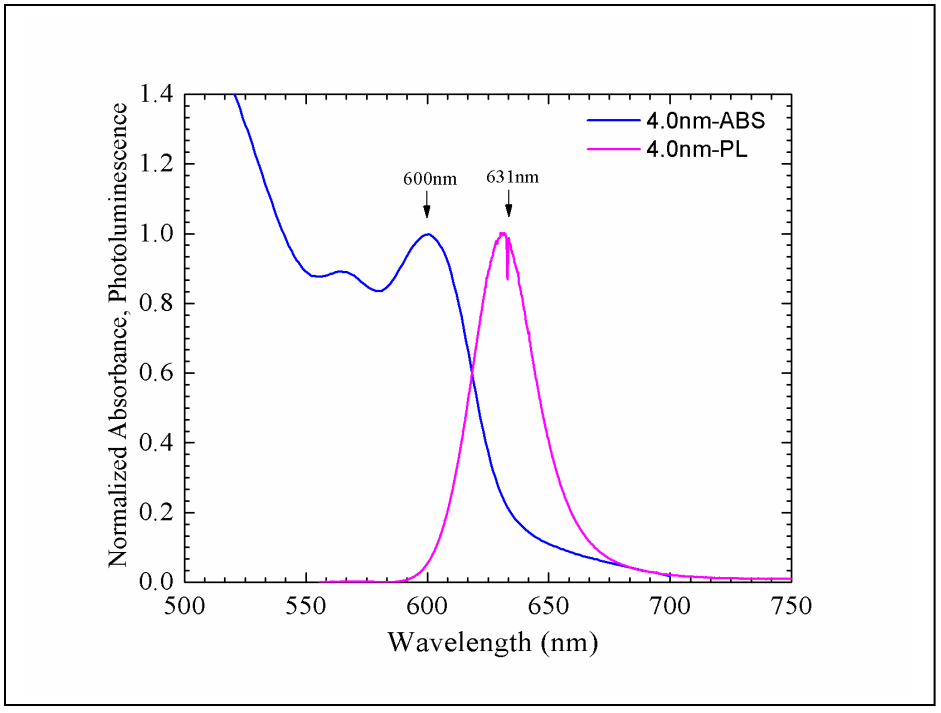

Figure 4.6 Normalized PL and absorption spectra are plotted together for the 4.0 nm nanocrystal diameter. The corresponding emission and the exciton peaks are labeled.

Because the emission spectrum is several orders of magnitude greater in intensity than the absorbance spectrum, the plots were normalized for comparison. In a similar fashion, Figures 4.5 and 4.6 display the absorbance and PL spectra for nanocrystal sizes of 3.2 and 4.0 nm respectively.

The differences in the first exciton peaks from the absorption spectra and the emission peaks from the PL spectra can be plotted as a function of the diameter of the nanocrystals. This plot is presented as Figure 4.7.

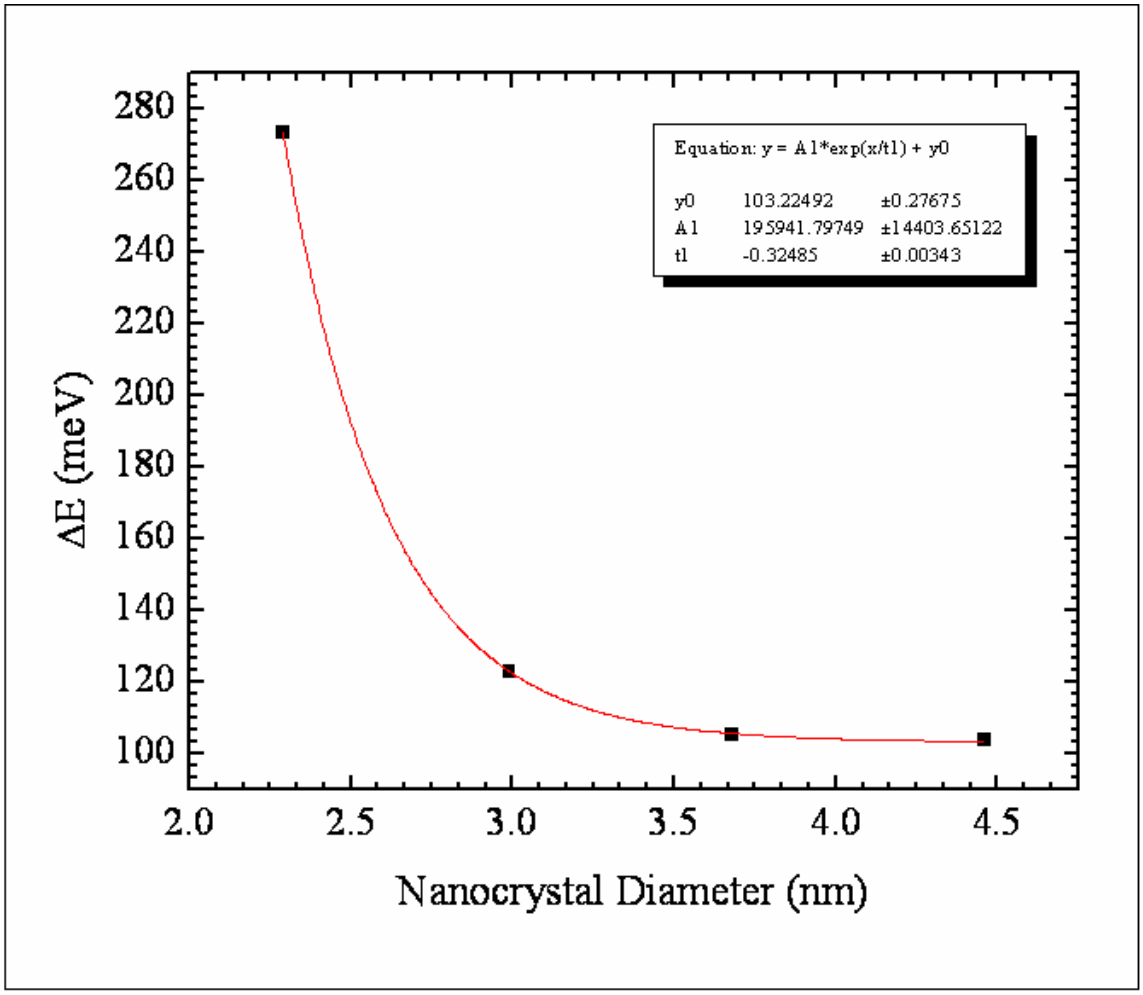

Figure 4.7 ΔE is plotted against nanocrystal diameter (indicated by black squares). The red solid line is an exponential fit of the data with the given equation.

The energy difference between the absorption and the PL peaks is known as the Stokes shift (ΔE). It can be expressed as:

$$\Delta E = 2S\hbar\omega_p$$

where, $\hbar\omega_p$ is the energy of the phonon coupled to the electron and

S is the Huang-Rhys factor.

The factor S gives an approximate estimate of the relative strength (or weakness) of the electron-phonon coupling. Just as in electromagnetic radiation, a photon is the smallest amount of quantized energy that can be emitted or absorbed, a phonon is the smallest discrete amount of quantized energy that occurs in vibration modes, such as vibration of atoms in a solid lattice. Larger values of S imply that the coupling is strong and vice-versa. Ref. 12 raises the possibility that one electron may be coupled to more than one phonon. If it is assumed that the electrons are coupled only to the LO phonon with energy $\hbar\omega_p$ = 25.0 meV, then the factors S are calculated as 2.08, 2.10, 2.46 and 5.46 for the quantum dot nanocrystals of size 4.5, 3.7, 3.0 and 2.3 nm respectively [12-14]. From Figure 4.7, it can be inferred that as the nanocrystal diameter decreases, the corresponding Stokes shift increases and the electron-phonon coupling increases as well.

4.5 Energy band gap as a function of temperature

As CdSe/ZnS core/shell nanocrystals fall under the category of wide band gap materials, the exciton binding energy is much smaller than the energy band gap (E_g). Hence, the energy band gap (E_g) can be approximated as the first exciton peak observed in the absorbance spectrum. Figure 4.8 represents the energy band gap plotted as a function of temperature for the four nanocrystal samples.

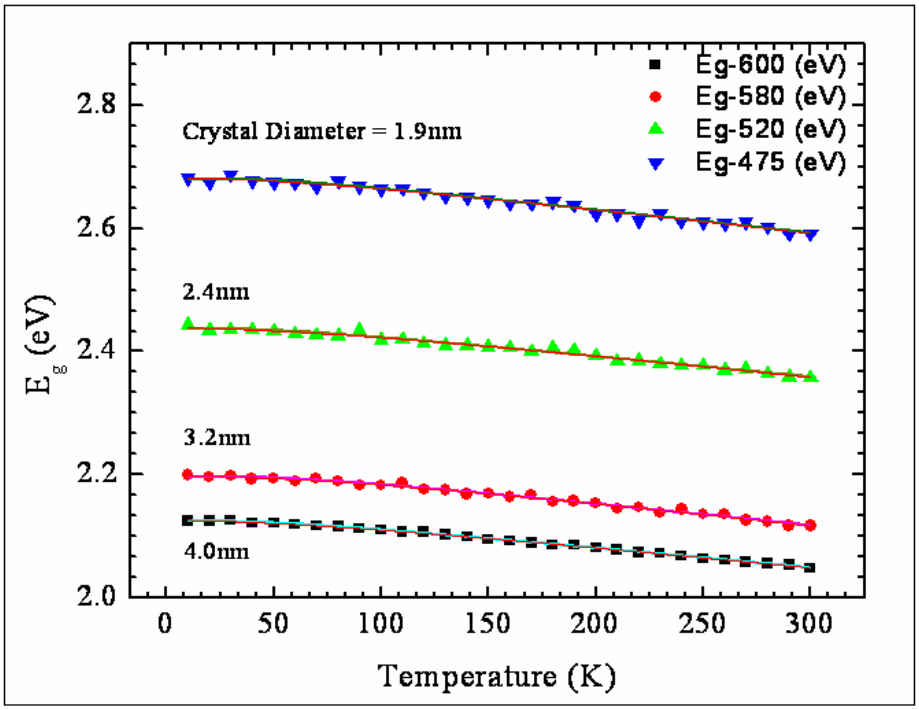

Figure 4.8 Energy band gap (E_g) is plotted as a function of temperature for the four nanocrystal samples.

It can be seen easily from this plot that as the nanocrystal temperature increases, the energy band gap decreases. The plots of these four nanocrystal samples were fit with the Varshni relationship [15]:

$$E_g(T) = E_g(0) - \frac{\alpha T^2}{T + \theta_D}$$

where $E_g(0)$ is the energy band gap at 0K, α is the temperature coefficient and θ_D is the 0K Debye temperature of the material. Both α and θ_D are used as fitting parameters and θ_D was found in the range of 130 – 195 K. The values for the Debye temperature agree with the work of other researchers (see Ref. [17]).

The energy band gap plot was also fitted with another empirical expression [16]:

$$E_g(T) = E_g(0) - \frac{\kappa}{\exp\left(\frac{\theta_E}{T}\right) - 1}$$

where $E_g(0)$ is the energy band gap at 0K, κ is a constant and θ_E is the Einstein temperature of the material. $E_g(0)$, κ and θ_E were used as fitting parameters and θ_E was found in the range 150-185K.

The values for θ_D and θ_E are summarized in Table 4.1 [12].

NC Diameter [nm]	$E_g(0)$ [eV]	α [10^{-4} eV/K]	Θ_D [K]	κ [10^{-2} eV]	Θ_E [K]	Θ_E/Θ_D
5.2	2.126	3.7±0.4	129±49	5.0±1.2	152±29	1.18
3.6	2.198	4.5±0.6	195±70	6.7±1.4	184±29	0.94
2.4	2.438	4.1±0.5	155±56	5.4±1.2	158±28	1.02
1.9	2.683	4.4±0.4	131±43	6.0±1.2	155±25	1.18

Table 4.1 Values of the parameters used in fitting the energy band gap equations to obtain the Debye and Einstein temperature values.

It can be deducted from the table that the ratio of Einstein temperatures to Debye temperatures is close to unity.

5. Conclusions

5.1 Summary of Important Points

The focus of this research work was to investigate the optical absorption and emission spectra from CdSe/ZnS colloidal core/shell nanocrystals. Four different CdSe/ZnS nanocrystal samples were made using a UV curable resin to create an embedded matrix of nanocrystal material. The four nanocrystal dot sizes were approximately 4.0, 3.2, 2.4 and 1.9 nm. The energy band gap (E_g), defined as the first exciton energy in the absorption spectrum, was observed to increase as the nanocrystal diameter decreased. The Stokes shift, obtained by computing the difference in the peaks in the absorption and emission spectra, was found to increase as the nanocrystal diameter decreases. The Huang-Rhys factor, S, was estimated for different samples with different nanocrystal diameters by assuming that there is coupling between the electron and phonon modes. This coupling was found to increase as the nanocrystal diameter decreased. The energy band gap (E_g) was also measured as a function of temperature and the energy band gap decreases as the temperature of the nanocrystal sample increases. Debye and Einstein temperatures were estimated by fitting the energy band gap as a function of temperature for different nanocrystal sizes with two empirical expressions. The ratio between the Einstein and the Debye temperatures was found to be approximately unity.

5.2 Future Work

The absorbance and emission (PL) spectra measurements from the colloidal CdSe/ZnS core/shell nanocrystals can be used to characterize the following devices:

- Solar Cells
- Light-emitting Diodes (LEDs)

Currently, a lot of research is being performed in the area of nanocrystals and the possibility to create high-efficiency solar cells and LEDs makes nanocrystals a very promising area to pursue research in.

6. References

[1] B. G. Streetman & S. K. Banerjee, Solid State Electronic Devices, Pearson Prentice Hall, 2006, Chapter 2, pp. 31-43.

[2] O. Manasreh, Semiconductor Heterojunctions and Nanostructures, McGraw-Hill, 2004.

[3] S. V. Gaponenko, Optical Properties of Semiconductor Nanocrystals, Cambridge University Press, 1998

[4] Semiconductor and Metal Nanocrystals, Victor I. Klimov, Marcel Dekker, 2004

[5] Al. L. Efros and A, L. Efros, Fiz. Tekh. Poluprovdn. **16**, 1209 (1982) [Sov. Phys. Semicond. **16.** 772 (1982)]

[6] L. E. Brus, J. Chem. Phys. **80,** 4403 (1984)

[7] D. J. Norris and M. G. Bawendi, Phys. Rev. B, **53**, 16338 (1996)

[8] A. Watt, T. Eichmann, H. Rubinsztein-Dunlop, and P. Meredith, Appl. Phys. Lett. **87**, 353109 (2005)

[9] Qing Shen and Taro Toyoda, Jpn. J. Appl. Phys., Part 1 **43**, 2946 (2004).

[10] J. Zhao, J. Zhang, C. Jiang, J. Bohnenberger, T. Basché, and A. Mews, J. Appl. Phys. **96**, 3206 (2004).

[11] Evident Technologies, On the World Wide Web: http://www.evidenttech.com

[12] A. Joshi, K. Y. Narsingi, M. O. Manasreh, E. A. Davis and B. D. Weaver, Appl. Phys. Lett. **89**, 131907 (2006).

[13] A. Brioude, J. Bellessa, S. Rabaste, B. Champagnon, L. Sphanel, J. Mugnier, and J. C. Plenet, J. Appl. Phys. **95**, 2744 (2004).

[14] M. C. Klein, F. Hache, D. Richard, and C. Flytzanis, Phys. Rev. B **42**, 11123 (1990).

[15] Y.P. Varshni, Physica **34**, 149 (1967).

[16] G. D. Cody, in *Hydrogenated Amorphous Silicon*, Semiconductors and Semimetals Vol. 21, edited by J. I. Pankove _Academic, New York, (1984), Pt. B, Chap. 2, pp. 11–79.

[17] D. Valerini, A. Cretí, M. Lomascolo, L. Manna, R. Cingolani, and M. Anni, Phys. Rev. B **71**, 235409 (2005).